Needle-based reflection refractometry of scattering samples using coherence-gated detection

Adam M. Zysk, Daniel L. Marks, Dianna Y. Liu[1], Stephen A. Boppart[2]

Biophotonics Imaging Laboratory, Beckman Institute for Advanced Science and Technology, Department of Electrical and Computer Engineering,
[2]Mills Breast Cancer Institute, Carle Foundation Hospital
University of Illinois at Urbana-Champaign, 405 North Mathews Avenue, Urbana, IL 61801, USA
[1]Current address: General Electric Healthcare, 9900 Innovation Drive, Wauwatosa, Wisconsin 53226, USA
boppart@uiuc.edu

http://biophotonics.uiuc.edu

Abstract: We present a novel method for *in situ* refractive index measurement of scattering samples using a needle device. The device employs a fiber-based reflectance refractometer and coherence-gated detection of the reflected optical signal that eliminates scattering-dependent backreflection contributions. Additionally, birefringence changes induced by fiber movement are neutralized by randomizing the source polarizations and averaging the measured Fresnel reflection coefficients over many incident polarization states. Experimental measurements of Intralipid scattering solutions are presented and compared with Monte Carlo simulations.

OCIS codes: (120.3180) Interferometry; (120.5710) Refraction; (160.4760) Optical Properties; (290.3030) Index Measurements.

References and links

1. S. Singh, "Refractive index measurement and its applications," Physica Scripta **65**, 167-180 (2002).
2. R. Barer, and S. Joseph, "Refractometry of living cells," Quarterly Journal of Microscopical Science **95**, 399-423 (1955).
3. J. Beuthan, O. Minet, J. Helfmann, M. Herrig, and G. Muller, "The spatial variation of the refractive index in biological cells," Phys. Med. Biol. **41**, 369-382 (1996).
4. A. Dunn, and R. Richards-Kortum, "Three-dimensional computation of light scattering from cells," IEEE Journal of Selected Topics in Quantum Electronics **2**, 898-905 (1996).
5. A. M. Zysk, E. J. Chaney, and S. A. Boppart, "Refractive index of carcinogen-induced rat mammary tumours," Phys. Med. Biol. **51**, 2165-2177 (2006).
6. A. M. Zysk, and S. A. Boppart, "Computational methods for analysis of human breast tumor tissue in optical coherence tomography images," J. Biomed. Opt. **11**, 054015 (2006).
7. H. A. Ferwerda, "The radiative transfer equation for scattering media with a spatially varying refractive index," J. Opt. A **1**, L1-L2 (1999).
8. L. Martí-López, J. Bouza-Domínguez, J. C. Hebden, S. R. Arridge, and R. A. Martínez-Celorio, "Validity conditions for the radiative transfer equation," J. Opt. Soc. Am. A **20**, 2046-2056 (2003).
9. J.-M. Tualle, and E. Tinet, "Derivation of the radiative transfer equation for scattering media with a spatially varying refractive index," Opt. Commun. **228**, 33-38 (2003).
10. H. Dehghani, B. Brooksby, K. Vishwanath, B. W. Pogue, and K. D. Paulsen, "The effects of internal refractive index variation in near-infrared optical tomography: a finite element modelling approach," Phys. Med. Biol. **48**, 2713-2727 (2003).
11. H. Dehghani, B. A. Brooksby, B. W. Pogue, and K. D. Paulsen, "Effects of refractive index on near-infrared tomography of the breast," Appl. Opt. **44**, 1870-1878 (2005).
12. M. Ohmi, Y. Ohnishi, K. Yoden, and M. Haruna, "In vitro simultaneous measurement of refractive index and thickness of biological tissue by the low coherence interferometry," IEEE Trans. Biomed. Eng. **47**, 1266-1270 (2000).
13. W. V. Sorin, and D. F. Gray, "Simultaneous thickness and group index measurement using optical low-coherence reflectometry," IEEE Photon. Technol. Lett. **4**, 105-107 (1992).

#80163 - $15.00 USD Received 16 Feb 2007; revised 1 Apr 2007; accepted 2 Apr 2007; published 5 Apr 2007

14. G. J. Tearney, M. E. Brezinski, J. F. Southern, B. E. Bouma, M. R. Hee, and J. G. Fujimoto, "Determination of the refractive index of highly scattering human tissue by optical coherence tomography," Opt. Lett. **20**, 2258-2260 (1995).
15. X. Wang, C. Zhang, L. Zhang, L. Xue, and J. Tian, "Simultaneous refractive index and thickness measurements of bio tissue by optical coherence tomography," J. Biomed. Opt. **7**, 628-632 (2002).
16. A. M. Zysk, J. J. Reynolds, D. L. Marks, P. S. Carney, and S. A. Boppart, "Projected index computed tomography," Opt. Lett. **28**, 701-703 (2003).
17. S. A. Alexandrov, A. V. Zvyagin, K. K. Silva, and D. D. Sampson, "Bifocal optical coherence refractometry of turbid media," Opt. Lett. **28**, 117-119 (2003).
18. A. V. Zvyagin, K. K. M. B. Dilusha Silva, S. A. Alexandrov, T. R. Hillman, J. J. Armstrong, T. Tsuzuki, and D. D. Sampson, "Refractive index tomography of turbid media by bifocal optical coherence refractometry," Opt. Express **11**, 3503-3517 (2003).
19. S. P. F. Humphreys-Owen, "Comparison of reflection methods for measuring optical constants without polametric analysis, and proposal for new methods based on the Brewster angle," Proceedings of the Physical Society **77**, 949-957 (1961).
20. G. H. Meeten, and A. N. North, "Refractive index measurement of absorbing and turbid fluids by reflection near the critical angle," Measurement Science and Technology **6**, 214-221 (1995).
21. A. M. Zysk, S. G. Adie, J. J. Armstrong, M. S. Leigh, A. Paduch, D. D. Sampson, F. T. Nguyen, and S. A. Boppart, "Needle-based refractive index measurement using low coherence interferometry," Opt. Lett. **32**, 385-387 (2007).
22. W. A. Reed, M. F. Yan, and M. J. Schnitzer, "Gradient-index fiber-optic microprobes for minimally invasive *in vivo* low-coherence interferometry," Opt. Lett. **27**, 1794-1796 (2002).
23. H. Ding, J. Q. Lu, K. M. Jacobs, and X. H. Hu, "Determination of refractive indices of porcine skin tissues and intralipid at eight wavelengths between 325 and 1557 nm," J. Opt. Soc. Am. A **22**, 1151-1157 (2005).
24. G. M. Hale, and M. R. Querry, "Optical constants of water in the 200-nm to 200-µm wavelength region," Appl. Opt. **12**, 555–563 (1973).
25. N. V. Iftimia, B. E. Bouma, M. B. Pitman, B. Goldberg, J. Bressner, and G. J. Tearney, "A portable, low coherence interferometry based instrument for fine needle aspiration biopsy guidance," Rev. Sci. Instrum. **76**, 064301 (2005).
26. M. Johns, C. A. Giller, D. C. German, and H. Liu, "Determination of reduced scattering coefficient of biological tissue from a needle-like probe," Opt. Express **13**, 4828-4842 (2005).
27. X. Li, C. Chudoba, T. Ko, C. Pitris, and J. G. Fujimoto, "Imaging needle for optical coherence tomography," Opt. Lett. **25**, 1520-1522 (2000).
28. G. J. Liese, W. Pong, and D. E. Brandt, "Fiber-optic stylet for needle tip localization," Appl. Opt. **24**, 3125-3127 (1985).
29. C. Zhu, G. M. Palmer, T. M. Breslin, F. Xu, and N. Ramanujam, "Use of a multiseparation fiber optic probe for the optical diagnosis of breast cancer," J. Biomed. Opt. **10**, 024032 (2005).
30. R. M. Pijnappel, M. van den Donk, R. Holland, W. P. T. M. Mali, J. L. Peterse, J. H. C. L. Hendriks, and P. H. M. Peeters, "Diagnostic accuracy for different strategies of image-guided breast intervention in cases of nonpalpable breast lesions," Br. J. Cancer **90**, 595-600 (2004).

1. Introduction

Refractive index measurement is important for a variety of scientific, medical, and industrial applications.[1] In biological systems, for example, refractive index variations are related to the protein and lipid concentrations in tissue[2] giving rise to variation of up to Δn=0.11 among sub-cellular structures.[3, 4] When considered along with the known morphological and molecular changes associated with disease progression, such as changes in protein concentration, the bulk refractive index may serve as a diagnostic indicator. In breast tissue, for example, recent research has shown that significant refractive index differences exist between the healthy adipose tissue comprising the majority of the breast and the diagnostically important epithelial and tumor tissues.[5] Knowledge of the bulk refractive index in these tissues is also key to understanding scattering processes that may be used for coherent[6] and diffuse tomographic imaging. Indeed, the spatial distribution of bulk refractive index in the breast has a significant effect on the reconstruction of diffusion tomography images due to the inherent dependence of the radiative transport equation on refractive index variation.[7-11]

Optical coherence tomography and low coherence interferometry (LCI) have been used extensively to measure the group refractive index of scattering samples by exploiting the sensitivity of interferometric pathlength measurements.[12-15] Measurement of the optical pathlength l through a sample with a known depth d yields the group refractive index

#80163 - $15.00 USD Received 16 Feb 2007; revised 1 Apr 2007; accepted 2 Apr 2007; published 5 Apr 2007

$n_g = l / d$. In addition to its use for bulk measurement, this method has been combined with direct and computed tomography techniques to form cross-sectional refractive index images.[16-18] In addition to precise pathlength sensing, coherent techniques may also be used map reflection amplitudes, a capability that enables the implementation of reflection refractometry techniques. Refractometry in scattering samples, however, is complicated by backscattered power from the sample, requiring *a priori* knowledge of the sample scattering coefficient.[19, 20] Spatiotemporal gating of the reflector position using low-coherence interferometry can eliminate this requirement and allow for measurement of the reflection intensity without regard for backscattering from the sample.

Despite the importance of tissue refractive index for imaging and diagnostic applications, no needle-based device capable of *in situ* refractive index measurement of scattering samples has been constructed at a size scale appropriate for clinical application. In this paper, we build upon previous needle measurement work[21] to develop a novel needle-based refractive index measurement technique. The device uses a simple fiber-based delivery system coupled to the sample arm of a low-coherence interferometer. This configuration enables coherence-gated reflectometry measurement of scattering samples at the probe-sample interface.

3. Materials and methods

The measurement device is a fiber-optic needle probe [22] connected to an LCI detection system consisting of SMF-28 fiber (*NA* = 0.11; Corning, Inc., Corning, New York) fused to a short length of graded-index multimode fiber (*NA* = 0.275, aperture = 62.5 μm; GIF625, ThorLabs, Newton, New Jersey). The micro-optics are enclosed within a 20-gauge stainless-steel hypodermic tube (HTX-20R, Small Parts, Inc., Miami Lakes, Florida) having a manufacturer-specified outer diameter of 0.914±0.013 mm and inner diameter of 0.457±0.051 mm. The tube end is ground to an angle of $\varphi_i = 36.6°$, as measured by light microscopy (Fig. 1). Finally, the end of the needle is filled with optical cement (NOA 65, Norland Products, Cranbury, New Jersey) and cured to form a flat surface. The outgoing beam maintains a spot size under 10 μm up to a distance of approximately 36 μm beyond the face of the multimode fiber, as calculated from

$$z \approx \frac{1}{\alpha}\cos\left(\frac{\lambda n_1}{r_s n_0 NA}\right), \tag{1}$$

where $\alpha = 2.93\times10^{-2}$ μm^{-1} is the focused beam angle, $\lambda = 1.3$ μm is the wavelength, r_s is the spot size, and $n_0 = 1.5$ and $n_1 = 1.42$ are the estimated refractive indices of the fiber and optical cement, respectively.

This device was coupled to the sample arm of the polarization sensitive LCI (PS-LCI) system shown in Fig. 2 via the SMF-28 single-mode optical fiber. The system included an SLD source (MenloSystems, Martinsried, Germany) with 1300 nm center wavelength and 75 nm bandwidth that yielded 5 mW of power incident on the sample and an axial resolution of 10 μm. A rapid-scanning optical delay (RSOD) performed fast axial scanning at 400 Hz. A polarization controller (P2) was used to align the RSOD polarization state with the state of maximum diffraction efficiency. A wavelength-independent lithium niobate polarization modulator (EOSpace, Inc., Redmond, Washington) consisting of a waveguide with single-mode fiber input and output connectors, and a modulator controller, was also included in the system. Optical circulators were used to avoid a double-pass through the modulator and enable dual-balance detection.

To perform refractometry measurements, the reflection intensity was measured at the interface between the needle tip optical cement seal and the tissue with which it was in contact. This measurement was performed via analysis of the LCI axial response averaged across both photodetectors. The reflection profile was windowed to include the axial region of the interface and exclude signal scattered from the interior of the sample, eliminating the need for *a priori* knowledge of the sample absorption and scattering properties, as is typical in reflection refractometry of turbid media.

#80163 - $15.00 USD Received 16 Feb 2007; revised 1 Apr 2007; accepted 2 Apr 2007; published 5 Apr 2007

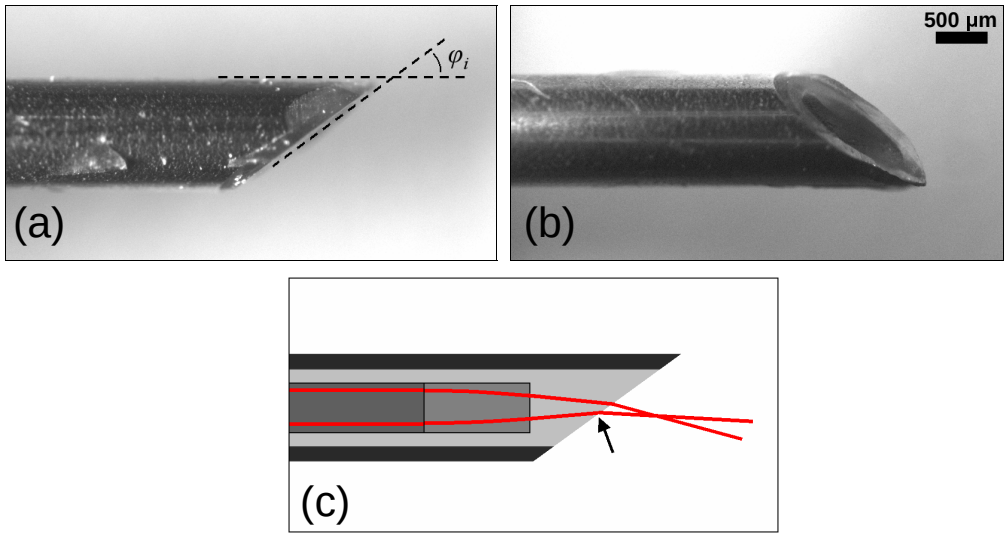

Fig. 1. Light microscope images of the needle tip show (a) the angled cutting surface and (b) the tip sealed with optical cement. The device drawing (c) shows the single mode and gradient-index fibers, the optical cement used to secure them, and the cement-sample interface (arrow) where the reflection amplitude is measured. The drawing is not to scale.

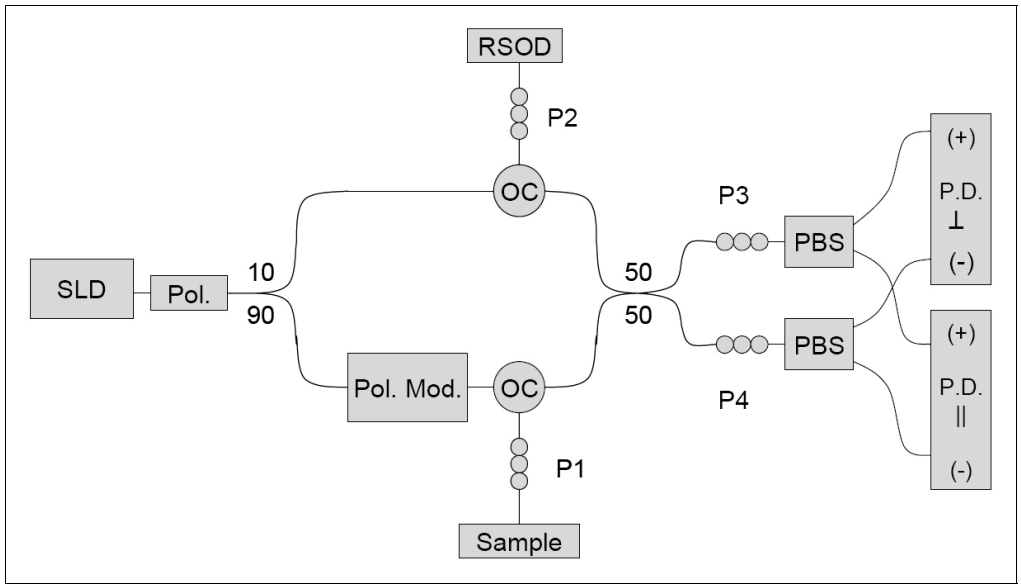

Fig. 2. Schematic of the PS-LCI system. Abbreviations: SLD, super luminescent diode; Pol., linear polarizer; Pol. Mod., polarization modulator; 90/10 and 50/50 fiber couplers; RSOD, rapid scanning optical delay; OC, optical circulator; P, polarization paddles; PBS, polarization beam splitter; P.D., photodetector.

In any handheld fiber-coupled probe, device movement is expected. In the case of this device, the polarization changes induced by this movement would likely induce significant reflection signal intensity fluctuations at the detector. This issue is addressed by introducing

#80163 - $15.00 USD Received 16 Feb 2007; revised 1 Apr 2007; accepted 2 Apr 2007; published 5 Apr 2007

random polarization variations in the polarization modulator fiber while recording the reflection coefficients. When generalized over the entire Poincaré sphere, the Jones vectors can be written

$$\begin{bmatrix} A_1 \\ A_2 \end{bmatrix} = \begin{bmatrix} \cos\theta & -\sin\theta \\ \sin\theta & \cos\theta \end{bmatrix} \begin{bmatrix} \frac{1}{\sqrt{2}} e^{i\phi/2} \\ \frac{1}{\sqrt{2}} e^{-i\phi/2} \end{bmatrix} = \frac{1}{\sqrt{2}} \begin{bmatrix} e^{i\phi/2}\cos\theta - e^{-i\phi/2}\sin\theta \\ e^{i\phi/2}\sin\theta + e^{-i\phi/2}\cos\theta \end{bmatrix}, \tag{1}$$

where ϕ and θ are the phase and polarization angle, respectively. The Fresnel reflection coefficient can, therefore, be written

$$\Gamma = \frac{1}{2}\left|e^{i\phi/2}\cos\theta - e^{-i\phi/2}\sin\theta\right|^2 \left|\Gamma_{\parallel}\right|^2 + \frac{1}{2}\left|e^{i\phi/2}\sin\theta + e^{-i\phi/2}\cos\theta\right|^2 \left|\Gamma_{\perp}\right|^2, \tag{2}$$

where

$$\Gamma_{\perp} = \frac{n_2\cos\varphi_i - n_1\cos\varphi_t}{n_2\cos\varphi_i + n_1\cos\varphi_t} \text{ and} \tag{3}$$

$$\Gamma_{\parallel} = \frac{n_1\cos\varphi_i - n_2\cos\varphi_t}{n_1\cos\varphi_i + n_2\cos\varphi_t}. \tag{4}$$

Here, n_1 and n_2 are the refractive indices of the optical cement and the tissue, respectively. The incident interface angle φ_i is the needle tip angle, and the transmitted interface angle is determined via the law of refraction

$$\varphi_t = \mathrm{Re}\left[\sin^{-1}\left(\frac{n_1}{n_2}\right)\sin\varphi_i\right]. \tag{5}$$

Figure 3 shows Monte Carlo simulations of the reflection intensity distribution over a uniform distribution of random polarization states. The results demonstrate that the use of mean reflection coefficients in this configuration is sufficient to accurately measure the sample refractive index.

#80163 - $15.00 USD Received 16 Feb 2007; revised 1 Apr 2007; accepted 2 Apr 2007; published 5 Apr 2007

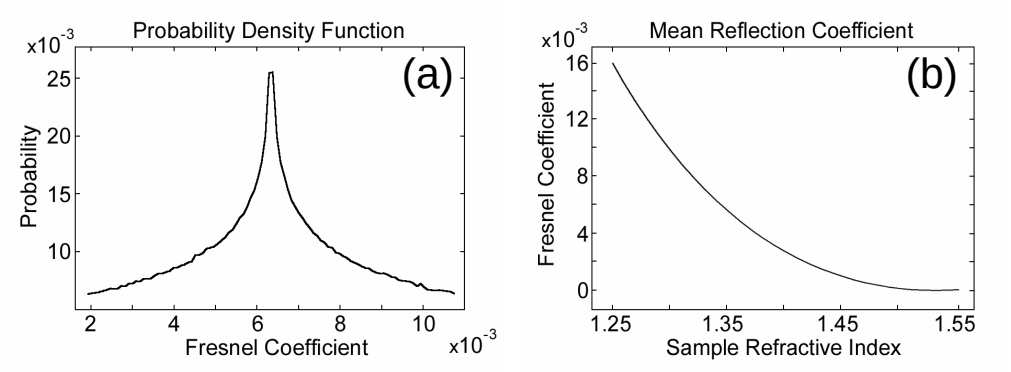

Fig. 3. Results of a Monte Carlo simulation of Eq. (2) with n_1 = 1.53 over N = 1×10^6 polarization states. (a) The distribution of Fresnel reflection coefficients for n_2 = 1.32. (b) The average Fresnel reflection coefficient for a range of n_2 values.

4. Results

To demonstrate refractive index and axial scattering measurements with this device, a set of scattering solutions were evaluated. One part Intralipid (10%) by volume was mixed with nine parts of a clear solution of glycerin and water. The ratio of glycerin to water was varied between samples, yielding solutions with different bulk refractive indices and uniform intralipid concentrations. Previously published refractive index values of these components are included in Table 1. The manufacturer-specified refractive index of the optical cement at visible wavelengths is $n_{1\ visible}$ = 1.524. The cement refractive index at the wavelength of operation was found to be n_1 = 1.515 by measuring clear solutions of glycerin and water, which were compared to simulated values from Eq. (2) using a least-squares fit.

Table 1. Refractive Indices of Measured Solutions

Sample	**Refractive Index**
Intralipid 10% [23]	1.34
Water [24]	1.322
Glycerin [21]	1.52

The axial scan data obtained from the scattering solutions demonstrated the expected uniform scattering response and exponential amplitude decay (see Figure 4). In each of the scattering solutions, $N = 1\times10^3$ axial responses were measured over 2.5 s of acquisition time while the incident polarization was randomized. The maximum reflection intensity in the axial region of the reflector was measured for each scan line yielding the distribution shown in Figure 5a. Mean values of the measured reflection amplitude for all solutions matched well with the expected values from simulation of equation (2) as shown in Figure 5b. The average error between the simulated and measured RI values was Δn = 0.0066 and the average percentage RI error was 0.46%. The number of unique polarization states (N_P) and the number of axial responses in each measurement influence the variance of the estimate, which decreases linearly by N/N_P. Repeated measurements within each sample yielded a low refractive index measurement standard deviation of ±0.0030 when averaged over all samples. This value is consistent with published reflection refractometry measurements in scattering media.[20]

#80163 - $15.00 USD Received 16 Feb 2007; revised 1 Apr 2007; accepted 2 Apr 2007; published 5 Apr 2007

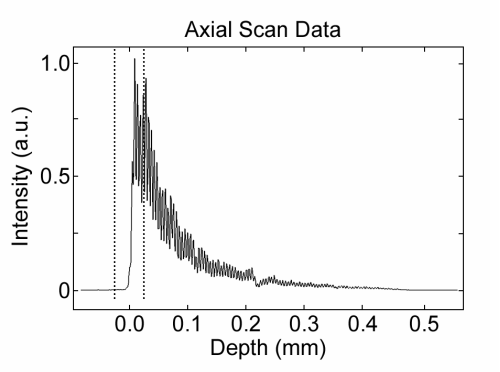

Fig. 4. Axial scan data from the needle probe averaged over 10 scan lines (25 ms acquisition time) while the probe tip is immersed in an Intralipid scattering solution with n_2 = 1.344. Dashed lines indicate the axial window of analysis.

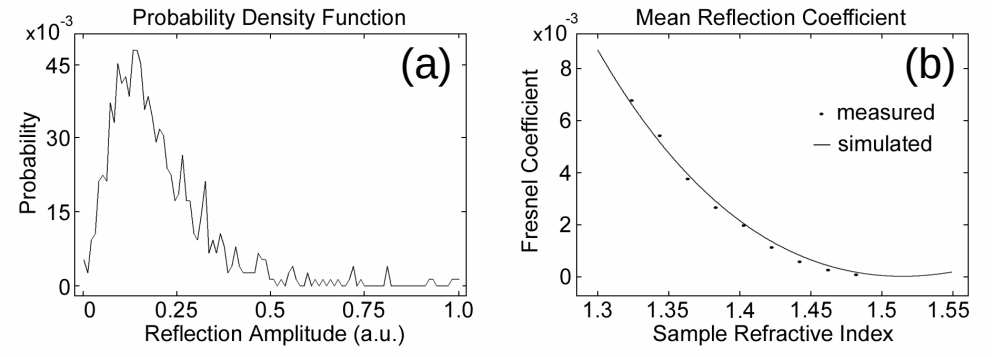

Fig. 5. Experimental measurements from scattering solutions. (a) The distribution of reflection amplitudes over N = 1×10^3 scan lines with incident light having a randomized polarization state. (b) Simulated Fresnel reflection coefficients averaged over N = 1×10^3 polarization states for a range of n_2 values and the corresponding mean reflection intensities for N = 1×10^3 scan line measurements in scattering solutions.

4. Discussion

In medicine, the localization and evaluation of disease often requires the use of forward sensing devices such as endoscopes, laparoscopes, and needles. Various optical sensing devices have been integrated into these clinical tools in order to enhance the applicable range of optical techniques. Scattering, spectroscopic, and fluorescence measurement instruments have been integrated into these device, often with the aim of guiding biopsy procedures or evaluating diseased tissue without excision.[25-29]

The results presented here have shown that needle-based refractive index measurement is also possible with a device appropriate for clinical application. Indeed, the size and construction of this device are compatible with commercially available 20 gauge core biopsy needle systems (Easy Core 20G, Boston Scientific, Natick, Massachusetts). The refractive index probe can be substituted for the cutting needle that is typically used to position a guide sheath prior to the insertion of the biopsy needle device. One possible application for this configuration is the guidance of needle biopsy procedures. Biopsy of breast lesions, for example, has a high non-diagnostic rate, often yielding samples that are insufficient for diagnosis.[30] The use of optical information from the site of the biopsy could potentially augment the current practices of localization via ultrasound or X-ray stereotaxis. The

#80163 - $15.00 USD Received 16 Feb 2007; revised 1 Apr 2007; accepted 2 Apr 2007; published 5 Apr 2007

refractive index of breast tissue is best understood by considering recently published measurements of rat mammary tumor tissue.[5] These data show refractive indices of n_t = 1.390±0.028, n_a = 1.467±0.026, and n_s = 1.388±0.043 for tumor, adipose, and stroma tissues, respectively. The difference between the adipose tissues that comprise the majority of the breast and the fibrous/tumor tissues of interest during a needle biopsy procedure is approximately 0.077 from mean-to-mean and 0.010-0.023 one standard deviation from the mean. The needle-based device presented here has a measurement accuracy that is appropriate for differentiation between these tissue types.

In conclusion, we have demonstrated needle-based refractive index measurements of scattering solutions. The use of axial reflection gating enabled reflection refractometry measurements without the need for *a priori* sample scattering information, and randomization of the incident polarization state eliminated motion-induced polarization effects that otherwise would have compromised measurement accuracy. The device size and construction are suitable for clinical use and future work is planned to evaluate the potential role of refractive index measurements in clinical applications.

Acknowledgments

We acknowledge a collaborative relationship with David D. Sampson and Steven G. Adie of the University of Western Australia that has yielded related results and has provided motivation for this work. We thank our clinical collaborators, Drs. Kendrith Rowland, Patricia Johnson, Jan Kotynek, and Frank Bellafiore at Carle Clinic Association and Carle Foundation Hospital, Urbana, Illinois, for their insights into the medical applications for this work. Finally, we acknowledge funding from the National Institutes of Health (Roadmap Initiative and NIBIB, 1 R21 EB005321 and 1 R01 EB005221, S.A.B.), the National Science Foundation (BES 03-47747 and BES 05-19920, S.A.B.), the Beckman Institute for Advanced Science and Technology, and Carle Foundation Hospital.

#80163 - $15.00 USD Received 16 Feb 2007; revised 1 Apr 2007; accepted 2 Apr 2007; published 5 Apr 2007